

JAERI-Research
2001-033



JP0150485



A STUDY OF FUEL FAILURE BEHAVIOR IN HIGH BURNUP HTGR FUEL
— ANALYSIS BY STRESS3 AND STAPLE CODES —

May 2001

David G.MARTIN*, Kazuhiro SAWA, Shouhei UETA
and Junya SUMITA

日本原子力研究所
Japan Atomic Energy Research Institute

本レポートは、日本原子力研究所が不定期に公刊している研究報告書です。
入手の問い合わせは、日本原子力研究所研究情報部研究情報課（〒319-1195 茨城県那珂郡東海村）あて、お申し越し下さい。なお、このほかに財団法人原子力弘済会資料センター（〒319-1195 茨城県那珂郡東海村日本原子力研究所内）で複写による実費頒布を行っております。

This report is issued irregularly.
Inquiries about availability of the reports should be addressed to Research Information Division, Department of Intellectual Resources, Japan Atomic Energy Research Institute, Tokai-mura, Naka-gun, Ibaraki-ken 〒319-1195, Japan.

A Study of Fuel Failure Behavior in High Burnup HTGR Fuel
- Analysis by STRESS3 and STAPLE Codes -

David G. MARTIN*, Kazuhiro SAWA, Shouhei UETA and Junya SUMITA

Department of HTTR Project
Oarai Research Establishment
Japan Atomic Energy Research Institute
Oarai-machi, Higashiibaraki-gun, Ibaraki-ken

(Received February 19, 2001)

In current high temperature gas-cooled reactors (HTGRs), Tri-isotropic coated fuel particles are employed as fuel. In safety design of the HTGR fuels, it is important to retain fission products within particles so that their release to primary coolant does not exceed an acceptable level. From this point of view, the basic design criteria for the fuel are to minimize the failure fraction of as-fabricated fuel coating layers and to prevent significant additional fuel failures during operation. This report attempts to model fuel behavior in irradiation tests using the U.K. codes STRESS3 and STAPLE. Test results in 91F-1A and HRB-22 capsules irradiation tests, which were carried out at the Japan Materials Testing Reactor of JAERI and at the High Flux Isotope Reactor of Oak Ridge National Laboratory, respectively, were employed in the calculation. The maximum burnup and fast neutron fluence were about 10%FIMA and $3 \times 10^{25} \text{ m}^{-2}$, respectively. The fuel for the irradiation tests was called high burnup fuel, whose target burnup and fast neutron fluence were higher than those of the first-loading fuel of the High Temperature Engineering Test Reactor. The calculation results demonstrated that if only mean fracture stress values of PyC and SiC are used in the calculation it is not possible to predict any particle failures, by which is meant when all three load bearing layers have failed. By contrast, when statistical variations in the fracture stresses and particle specifications are taken into account, as is done in the STAPLE code, failures can be predicted. In the HRB-22 irradiation test, it was concluded that the first two particles which had failed were defective in some way, but that the third and fourth failures can be accounted for by the pressure vessel model. In the 91F-1A irradiation test, the result showed that 1 or 2 particles had failed towards the end of irradiation in the upper capsule and no particles failed in the lower capsule.

Keywords: HTGR, Coated fuel particle, Failure, High burnup, Irradiation test,
Pressure vessel model

* Nuclear Fuels Consultant to AEA Technology (stayed at the Department of HTTR Project as an invited foreign researcher from March to April 2000)

高温ガス炉燃料の高燃焼度下における破損挙動の研究
- STRESS3 コード及び STAPLE コードによる解析 -

日本原子力研究所大洗研究所高温工学試験研究炉開発部
David G. MARTIN* · 沢 和弘 · 植田 祥平 · 角田 淳弥

(2001 年 2 月 19 日受理)

現在の高温ガス炉では四重被覆燃料粒子を燃料として用いている。高温ガス炉燃料の安全設計においては、1 次冷却材への放出量が許容値を超えないよう、核分裂生成物を被覆燃料粒子内に閉込めることが重要である。この観点から、燃料に対する設計の基本方針は、製造時の破損を最小化すること及び運転中の著しい追加破損を防止することである。本報は、高燃焼度下における燃料挙動の研究のため、照射試験中の燃料挙動を英国のコード STRESS3 と STAPLE を用いて再現しようと試みた結果を示す。計算には、原研の JMTR において 91F-1A キャプセルで、ORNL の HFIR において HRB-22 キャプセルで実施した照射試験結果を用いた。最高燃焼度及び高速中性子照射量はそれぞれ約 10%FIMA、 $3 \times 10^{25} \text{ m}^{-2}$ であった。これらの試験では、高燃焼度燃料と呼ばれる、高温工学試験研究炉初装荷燃料よりも目標燃焼度及び高速中性子照射量を高く設定して設計した燃料を照射した。まず、PyC 及び SiC 層の平均破壊強度を用いて計算すると、破損は生じないという結果が得られた。一方、STAPLE コードで被覆層の破壊強度及び厚さを統計的に取扱うと、破損挙動を再現できた。HRB-22 キャプセル照射試験では、追加破損のうち始めの 2 粒子の破損は被覆層に欠陥のある粒子の破損であり、3、4 番目の破損は内圧上昇に伴うものであると結論した。91F-1A キャプセルでは、上段で 1~2 粒子、下段で破損しないという結果を得た。

大洗研究所：〒319-1394 茨城県東茨城郡大洗町成田町新堀 3607

* Nuclear Fuels Consultant to AEA Technology (2000 年 3 月から 4 月に外国人研究者招聘制度により高温工学試験研究炉開発部に滞在)

Contents

1. Introduction	1
2. Analytical Model	2
2.1 Principal Features	2
2.2 Features of the Code	2
2.3 Outline of Mathematical Basis of STRESS3	3
2.4 Modeling the Failure of a Layer	4
2.5 Calculation of Gas Pressure	4
2.6 Statistical Evaluation	4
3. Irradiation Data for Analysis	5
3.1 Capsule Design	5
3.2 Fission Gas Release	5
3.3 Failure Fraction	5
4. Results and Discussions	7
4.1 HRB-22 Capsule Irradiation Test	7
4.2 91F-1A Capsule Irradiation Test	9
5. Conclusions	11
Acknowledgement	12
References	12

目 次

1. はじめに	1
2. 解析モデル	2
2.1 基本モデル	2
2.2 コードの特徴	2
2.3 STRESS3 コードのモデルの概要	3
2.4 被覆層破損のモデル	4
2.5 内圧ガスの計算	4
2.6 統計的評価	4
3. 解析に用いた照射データ	5
3.1 キャプセル設計	5
3.2 核分裂生成物ガス放出	5
3.3 破損率	5
4. 結果及び考察	7
4.1 HRB-22 キャプセル照射試験	7
4.2 91F-1A キャプセル照射試験	9
5. 結論	11
謝辞	12
参考文献	12

1. INTRODUCTION

In current high temperature gas-cooled reactors (HTGRs), Tri-isotropic (TRISO)-coated fuel particles are employed as fuel. The TRISO coatings consist of a low-density, porous pyrolytic carbon (PyC) buffer layer adjacent to the spherical fuel kernel, followed by an isotropic PyC layer (inner PyC; IPyC), a silicon carbide (SiC) layer and a final PyC (outer PyC; OPyC) layer as shown in Fig. 1. In safety design of the HTGR fuels, it is important to retain fission products within particles so that their release to primary coolant does not exceed an acceptable level. From this point of view, the basic design criteria for the fuel are to minimize the failure fraction of as-fabricated fuel coating layers and to prevent significant additional fuel failures during operation^(1,2).

This report attempts to model additional failures in the two capsules using the U.K. codes STRESS3 and STAPLE⁽³⁾. STRESS3 code calculates stresses in all the layers of a specific particle design over the course of its irradiation, and, if appropriate, models the failure of layers when stresses in them exceed their fracture stresses. By contrast, STAPLE code is a statistical model. It performs many STRESS3 runs on particles selected randomly in accordance with their manufacturing variability and the variability in the failure stresses of each layer.

The calculations were carried out for 91F-1A and HRB-22 capsule irradiation tests. The fuel for the irradiation tests were called high burnup fuel, whose target burnup and fast neutron fluence were higher than those of the first-loading fuel of the High Temperature Engineering Test Reactor (HTTR). In order to keep fuel integrity up to high burnup over 5% FIMA (% fission per initial metallic atom), thickness of buffer and SiC layers of fuel particle were increased⁽⁴⁾. The fuel compacts were irradiated in the 91F-1A and HRB-22 capsules at the Japan Materials Testing Reactor (JMTR) of JAERI, and at the High Flux Isotope Reactor (HFIR) of Oak Ridge National Laboratory (ORNL), respectively. During the irradiation tests, additional through-coatings failures of coated fuel particles were observed⁽⁵⁾. The pressure vessel failure model developed by JAERI was applied to account for these failures⁽⁴⁻⁶⁾. However, since the model predicted that the SiC layer always remained under compression throughout the course of the irradiation it was unable to account for these failures. In view of this conclusion it was proposed that particle coatings could completely fail if the SiC layer became defected during manufacture since evidence was presented which suggested that under these circumstances the PyC layers of a small fraction of the particles could fail during the irradiation.

2. ANALYTICAL MODEL

STRESS3 code evaluates the stresses and strains of coating layers in a sequence of consecutive neutron dose steps. The failure and de-bonding of the layers can be modeled, and irradiation simulated until all the layers (not just the SiC layer) have failed. Virtually all material properties can be specified as varying with the neutron dose and realistic irradiation histories, including shut downs, can be handled. Stresses on the coating layers due to kernel - buffer mechanical interactions as well as those due to internal gas pressure can be dealt with. Moreover, any combination of layers, up to a maximum of 6 can be modeled. After each neutron dose step, information relating to the tangential stress and creep strain in each layer, the radial stress between layers and, if de-bonding has occurred, the gap size between the two is quoted. In addition, values of the internal void and gas pressure and also the change in diameter of the whole particle are printed.

2.1 Principal Features

- (1) Evaluates stresses and strains in a sequence of consecutive finite time steps. Values are known at the beginning of the step. Values of stress and strain changes, $\Delta\sigma$ and $\Delta\varepsilon$, over each time step are calculated.
- (2) A differential equation in, essentially, $\Delta\varepsilon$ (actually change of displacement, Δu) for each layer is set up and solved, using a stable, accurate method, plus the imposition of appropriate boundary conditions between the layers.
- (3) Calculation of gas pressure and void is performed iteratively (Of especial importance if the SiC layer has failed).
- (4) Spherical symmetry is assumed - but not believed to be a fundamental limitation.

2.2 Features of the Code

- (1) Virtually all material properties can be defined as functions of the neutron dose.
- (2) All known factors affecting particle endurance are incorporated.
- (3) Realistic irradiation histories can be specified.
- (4) The calculation does not have to rely on the assumption that the SiC layer is rigid.
- (5) Kernel - buffer mechanical interactions can be modeled.
- (6) Failure criteria for each of the layers can be specified.
- (7) Possible de-bonding of the layers can be modeled.
- (8) Irradiation can be modeled until all the layers (not just the SiC layer) have failed.

- (9) Any combination of layers (currently up to a maximum of 6) can be modeled.
- (10) The output after each time step includes information on:
- Tangential stress and creep strain in each layer.
 - Radial stress between layers and, if de-bonding has occurred the size of gap between the two.
 - Internal void and gas pressure.
 - The change in diameter of the whole particle.
 - Report of whenever layers fail, or de-bonding occurs.

2.3 Outline of Mathematical Basis of STRESS3^(3,7)

During the current time step changes in stresses and strains $\Delta\sigma$ and $\Delta\varepsilon$ are required. The change in strain during this neutron dose step is given by as follows.

$$\Delta\varepsilon_1 = \sum_{m=1}^3 \left[\underbrace{E_{lm} \Delta\sigma_m}_{\text{elastic}} + \underbrace{K_{lm} \left(\sigma_m + \frac{1}{2} \Delta\sigma_m \right) \Delta\phi}_{\text{irradiation creep}} + \underbrace{C_{lm} \left(\sigma_m + \frac{1}{2} \Delta\sigma_m \right) \Delta\tau}_{\text{thermal creep}} \right] \\ + \underbrace{T_1 \Delta\theta}_{\text{thermal expansion}} + \underbrace{G_1 \Delta\phi}_{\text{irradiation induced dimensional change}} + \underbrace{Z_1 \Delta\tau}_{\text{thermally induced dimensional change}} \quad (1)$$

The relation between radial displacements, u , and the tangential and radial strain at a radial coordinate x is

$$\Delta\varepsilon_1 = \frac{\Delta u}{x} ; \quad \Delta\varepsilon_3 = \frac{d\Delta u}{dx} . \quad (2)$$

The equation of equilibrium is

$$\Delta\sigma_1 = \Delta\sigma_3 + \frac{1}{2} x \frac{d\Delta\sigma_3}{dx} . \quad (3)$$

Eliminating $\Delta\varepsilon_1$, $\Delta\varepsilon_3$, $\Delta\sigma_1$ and $\Delta\sigma_3$ gives a differential equation in Δu .

$$x^2 \frac{d^2 \Delta u}{dx^2} + 2x \frac{d\Delta u}{dx} - 2\gamma \Delta u = 2(\delta + \xi)x , \quad (4)$$

where γ , δ , ξ are expressions derived from the material properties and other variables. γ and δ are constants, whereas ξ is a function of x since it depends on the known stresses at the start of the step.

The solution, which includes a complementary function and a particular integral, contains two constants of integration, which are defined by the boundary conditions between the layers.

2.4 Modeling the Failure of a Layer

If the fracture stress is exceeded at the end of a step, a number of pseudo-time steps are introduced which involve (thermal) creep relaxation until the tangential stress becomes essentially zero. During subsequent steps tangential elastic compliance constants (E_{11} and E_{12}) are set extremely high to ensure tangential stresses in the layer remain low.

2.5 Calculation of Gas Pressure

The voidage within which those regions of the particle into which gas can permeate is calculated. This includes the open porosity in the kernel and all the porosity in the buffer, since this is assumed to be open and so can be occupied by gas.

The amount of gas created by fission, namely Xe, Kr, CO and CO₂ is evaluated and the gas pressure then calculated using an appropriate equation of state. This calculation must be performed iteratively because gas pressure and voidage are inter-related.

2.6 Statistical Evaluation

STRESS3 code is a useful tool for calculating the values of many variables relating to a particle with a specific design over the course of its irradiation. However, in addition, one is also concerned with the irradiation of a batch of particles, each of which does not possess a set of identical specifications, in particular in knowing what fraction has failed after a specific burnup. The computer code STAPLE (STATistics of Particle Life) is able to provide such information. It selects particles randomly with specifications that are in keeping with their manufacturing tolerances, performs on each a STRESS3 run in order to determine the burnup at which failure occurs and then stores this value. The following parameters can be assumed to be normally distributed and their 1σ standard deviation specified.

- kernel diameter
- thickness of each coating layer
- open porosity in the kernel and coating layers
- closed porosity in the kernel

In addition, the fracture stresses of any of the layers can be made to obey Weibull statistics.

3. IRRADIATION DATA FOR ANALYSIS

The fabricated high burnup fuel compacts were irradiated in two capsules, 91F-1A capsule and HRB-22 capsule. The irradiation and post-irradiation examination were independently carried out. The 91F-1A capsule and the HRB-22 capsule were irradiated at JMTR in JAERI and at HFIR in ORNL^(4,8-10). The measured dimensions, including their deviation, of the irradiated coated fuel particles are shown in **Table 1**.

3.1 Capsule Design

The HRB-22 capsule consisted of a doubly contained, single purge cell with 12 fuel compacts held in a graphite fuel body. The twelve compacts were enclosed in a fuel body. Capsule temperatures were adjusted by changing the composition of the sweep gas flowing in the gap between the graphite fuel body and the inconel pressure vessel. The 91F-1A irradiation rig consisted of two capsules, upper and lower, which were irradiated and monitored independently. Each capsule contained two fuel compacts. Temperatures were controlled by adjusting the gas pressure between the two walls. Burnups and fast neutron fluences for the fuel compacts are shown in **Figs. 2 and 3**, respectively. The fuel temperatures were evaluated based on measured TC temperatures. Time-dependent maximum fuel temperatures are shown in **Fig. 4**. The maximum values of twelve fuel compacts are shown for the HRB-22 capsule irradiation test.

3.2 Fission Gas Release

The release rate-to-birth rate ratio (R/B) is an important measure of the performance of the coated particle fuel. In the 91F-1A irradiation test, sweep gas was sampled from both inner capsules independently. The measured (R/B) values were shown in **Fig. 5** during HRB-22 and 91F-1A capsule irradiation tests.

3.3 Failure Fraction

The comparison of measured and calculated (R/B)s during the HRB-22 capsule irradiation test is shown in **Fig. 6**. At the beginning of irradiation between 0 to 30 EFPD (Effective Full Power Days), when no additional failure occurred, the fractional release varies in accordance with change of the fuel temperature. The calculated results give relatively good agreement with the measured (R/B)s when there were two through-coatings failed particles at the beginning of irradiation. Since there were 3.2×10^4 of the fuel particles in the HRB-22

capsule, the failure fraction was 6.3×10^{-5} at the beginning of irradiation. The failure fraction reached to 1.9×10^{-4} at the end of irradiation because additional fuel particle failures were observed at 30.4, 32.6, 59.7 and 83.3 EFPDs (Effective Full Power Days) by the ionization chamber monitoring during irradiation. In the calculation, the uranium contamination fraction of 2×10^{-6} was employed.

Increase of fractional release by the first (30.4 EFPD) and the second (32.6 EFPD) failures was clearly observed in the measurement, and the calculated fractional releases show good consistency with the measured data. On the other hand, since the third and fourth failures occurred when the fuel temperature decreases, no clear increase of release fraction was observed.

Figure 7 shows the comparison of measured and calculated (R/B)s during the 91F-1A capsule irradiation test. It is evaluated that there is no through-coatings failed particle at the beginning of irradiation, then fission gas is released from matrix contaminated uranium (fraction is estimated to be 2×10^{-6}). At the end of irradiation, the through-coatings failure fraction is evaluated to be about 5×10^{-5} , which corresponds to 0 or 1 particle failure in each inner capsule. The postirradiation examination was also carried out to evaluate failure fraction. The free uranium fraction of the irradiated fuel compacts was measured by the deconsolidation followed by the acid leaching on three fuel compacts (two from upper, one from lower). The solution was analyzed for uranium by fluorometric analysis. The measured values showed that 1 or 2 through-coatings failed particles were present in a upper fuel compact which contained about 5000 coated fuel particles. Other two fuel compacts did not contain the through-coatings failed particle. The measured free uranium fraction ($=$ (uranium in solution) / (uranium in a fuel compact)) were about $2 \sim 4 \times 10^{-4}$.

4. RESULTS AND DISCUSSIONS

4.1 HRB-22 Capsule Irradiation Test

According to the JAERI pressure vessel model, the SiC layer remained under compression throughout the entire irradiation⁽³⁾. This was indeed confirmed again in the present analysis. In fact the STRESS3 run was extended to very high burnup and it was found that stresses in the SiC layer were only tensile when burnup achieved 12%FIMA or higher. Quite simply, at neutron doses relevant to those of the HRB-22 irradiation, attempted shrinkage of the PyC layers provides compressive stress components which more than cancel out the tensile stress component due to the internal gas pressure. The only possible way by which stresses in the SiC layer can become tensile at neutron doses relevant to the irradiation is if at least one of the PyC layers has failed first. However this does not seem likely because the tensile stress in either PyC layer never exceeds 132 MPa throughout the course of the irradiation, which is well below most, if not all, mean fracture stresses that have been reported for high density isotropic PyC (But this comment will be modified when the statistics of particle failure are considered - see below.).

However, in order to investigate whether the premature fracture of one or both PyC layers could result in the SiC layer becoming sufficiently stressed in tension that its failure became possible, a sequence of three STRESS3 runs were performed. In the run that was described above the fracture stress of both PyC layers was set at 400 MPa. In the first of a sequence of three, the run was repeated but with the IPyC fracture stress lowered to 50 MPa, so that this layer failed early in life. It was found that stresses in the SiC layer only became tensile at 6.8%FIMA, rising to 59 MPa at 12%FIMA. In the second run the fracture stress of just the OPyC layer was lowered to 50 MPa. Stresses in the SiC layer became tensile at a burnup of 5.8%FIMA, increasing with burnup to 114 MPa at 12%FIMA. For the third run the fracture stresses of both the IPyC and OPyC layers were lowered to 50 MPa. Because both PyC layers failed very early in life the SiC layer was in tension over nearly the whole of the irradiation. Nevertheless, while the stress in the SiC layer rises monotonically with burnup, it has only attained 90 MPa even at the end of irradiation, rising to 173 MPa at 12%FIMA. It is concluded therefore that on the basis of our knowledge of the mean fracture stress values of PyC and silicon carbide it is difficult to predict failure of all the layers. Even if both PyC layers fail prematurely, the build-up of internal gas pressure at 7%FIMA seems inadequate to stress the SiC layer sufficiently to cause it to fail, given our current knowledge of the mean fracture stress of SiC.

The above discussion is based entirely on mean fracture stress values for the various layers. It is well known that SiC, being a brittle material, fails in accordance with Weibull statistics. There is experimental evidence which indicates that PyC also fails by Weibull statistics, i.e. that the fraction of layers which have failed, f , when subject to a stress σ is given by the relation

$$f = 1 - \exp \left\{ - \ln 2 \left(\frac{\sigma}{\sigma_0} \right)^m \right\}, \quad (5)$$

where σ_0 is the mean fracture stress, corresponding to $f=0.5$, and m is a constant.

Experimental values of σ_0 for both SiC and PyC are quite variable. In the case of SiC it is known that slow deposition rates, thereby minimizing surface flaws, are able to raise its value quite substantially. A number of bend test measurements on PyC layers have been reported, largely by General Atomic workers. However their results are not directly applicable to whole coating layers. Appropriate σ values have been obtained by Bongartz *et al.*⁽¹¹⁾ who, for high density isotropic PyC layers have derived values for σ_0 and m in the ranges 180-220 MPa and 5-7 respectively. A review of all this data may be found in Ref. 12.

Given these observations, it would appear reasonable to assume that $\sigma_0=200$ MPa for all three load bearing layers and to choose values for m ranging between 5 and 7. **Figure 8** shows failure probabilities relating to m values of 5, 6, 7 and a σ_0 value of 200 MPa. It is evident that at a stress of 50 MPa failure fractions in the region of 10^{-3} to 10^{-4} occur, which is comparable to the fraction actually observed.

The code STAPLE was then run with all the variations in dimensions of the particle that were listed in **Table 1**, together with the Weibull failure statistics. For each of the three cases considered, with m values of 5, 6, and 7 respectively, 32,000 runs of STRESS3, corresponding to the number of fuelled particles contained in the compacts, were performed. The number of failed particles as a function of burnup at values for which particles begin to fail is shown in **Fig. 9**. This shows that in the case of $m=5$ the first four failures occur at burnup of 6.125, 6.625 and 7.375%FIMA (2). When $m=6$ the corresponding values are 6.125, 7.375, 8.125 and 8.375%FIMA, while for $m=7$ they are 6.375, 8.125 (2) and 8.375%FIMA. Clearly when these results are compared with the experimental values the $m=5$ results provide the best agreement and these will be discussed below.

The STAPLE results have shown that by the time that 7% burnup has been reached four particles have very nearly failed. Clearly better agreement could be attained by fine tuning the value of m , and possibly also σ_0 , but this is hardly necessary.

However the shortcoming of this correlation is it ignores the fact that two of the failures occurred after about 30 EFPDs, when burnup were in the region of around 2.6%FIMA. It would appear that if we assume that all particles matched their specifications then it is not possible, on the basis of a pressure vessel model, to account for these two failures. If these are ignored, then the third and fourth particles which failed at 59.7 and 83.3 EFPDs may be correlated with the first two failures of the STAPLE run at 6.125 and 6.625%FIMA.

The only explanation remaining for the first two failures would appear to assume that in some way these particles were defective. The suggestion that they possessed defective silicon carbide layers made in Ref. 4 is one possible explanation for these failures. The difficulty is that we do not know either the number of such particles nor the exact details of the defects, which would be necessary if they were to be modeled.

One way forward, had this been a possibility, would have been to continue the irradiation and observe the rise in the number of failed particles with burnup. Presumably the failures due to defective particles would form a tail at low burnup before the build-up in the number failed due to pressure vessel failure of normal particles takes place, as the burnup increases.

It is concluded that the first two particles which failed were defective in some way but that the third and fourth failures can be accounted for by the pressure vessel model.

4.2 91F-1A Capsule Irradiation Test

(1) Upper Capsule Results

Initially a sequence of STRESS3 runs were performed. The first employed reasonably high fracture stresses for each of the three load bearing layers (IPyC, SiC and OPyC), namely 400MPa. These results indicated that up to 8%FIMA, stresses in the SiC were always compressive, and that neither of the PyC layers had failed. Clearly, therefore, if failure of all three load bearing layers is to be modeled, one or both PyC layers must fracture first. Accordingly, three further STRESS3 runs in which, by setting the fracture stress of a PyC layer equal to 50 MPa, it was made to fail early in life. It was found that if the IPyC layer were made to fail prematurely the stress in the SiC layer at 8%FIMA was now tensile, but with a value of only 25 MPa. When the OPyC layer was made to fail, the corresponding stress increased slightly to 36MPa, whereas if both IPyC and OPyC failed prematurely the tangential stress in the SiC layer at 8%FIMA was 125MPa. Clearly, therefore, failure of all three load bearing layers is most likely to occur if both the IPyC and OPyC layers could be made to fail first.

In order to explore this possibility, a STAPLE run was performed, using the variations in particle thickness presented in **Table 1** and applying to all three load bearing layers Weibull failure statistics given by equation (5). On the basis of the HRB-22 irradiation experiment described above, we will assume a mean failure stress of 200MPa and $m=5$ for all three load bearing layers.

4,400 particles were present in the compact. However, in order to obtain better statistics, ten times this number was employed in the calculation. **Figure 10** shows the number of calculated failed particles as a function of burnup and demonstrates that 1 and 2 failures occurred at about 7.5 and 8%FIMA, in reasonable agreement with observations that 1-2 particles had failed towards the end of irradiation.

(2) Lower Capsule Results.

STRESS3 and STAPLE runs were performed in a manner analogous to those relating to the upper capsule. However, in this case it was found, from the STRESS3 results, that the SiC layer was only in tension at 9.5%FIMA when both PyC layers had failed, when the stress was 67MPa. If one or both PyC layers remain intact throughout the irradiation, the SiC layer was always under compression. The comparatively low stress in the SiC layer, even when both PyC coatings have failed, implies that failure of all three load bearing layers is less likely compared with the upper capsule. A STAPLE run, using the same failure statistics as were employed with the upper capsule indeed confirmed this. It showed that the first failure (corresponding, as explained above, to 10 calculated failures) only occurred at a burnup of 11.75%FIMA, which is significantly higher than the end of life burnup value. This is in keeping with the observation that no particles failed during irradiation.

It appears that no failures were observed in the comparatively more highly rated lower capsule because, from about half way through the irradiation, the temperature decreased continually with increasing burnup. By contrast, though comparatively lower rated, the upper capsule experienced failures because irradiation temperatures were maintained. One reason why the lower capsule irradiation has been modeled successfully is because STRESS3 and STAPLE are able to handle various properties and parameters, including temperature and fission gas release fraction, which vary continually with irradiation time.

Perhaps one of the more satisfying findings of the present study is that it has proved possible to use the same mean fracture stress and m values that were employed in the HRB-22 modeling exercise. So, on the basis of these two studies, the tentative conclusion is that a consistent set of data has been produced which can be used for the modeling of future JAERI irradiation tests.

5. CONCLUSIONS

The analysis was carried out to investigate failure behavior by the U.K. codes STRESS3 and STAPLE.

1. The first STRESS3 run showed that the SiC layer remained under compression throughout the entire irradiation. The result was consistent with the result obtained by the JAERI model.
2. In order to investigate whether the premature fracture of one or both PyC layers could result in the SiC layer, the fracture stress of both PyC layers was changed in the calculation. It is concluded that on the basis of our knowledge of the mean fracture stress values of PyC and silicon carbide it is difficult to predict failure of all the layers.
3. The code STAPLE runs with all the variations in dimensions of the particle and the Weibull failure statistics for the HRB-22 irradiation test. It was concluded that the first two particles which failed were defective in some way but that the third and fourth failures can be accounted for by the pressure vessel model.
4. The failures in the upper capsule and the absence of failures in the lower capsule of the 91F-1A irradiation were modelled successfully using the STAPLE code. It has proved possible to use the same mean fracture stress and m values that were employed in the HRB-22 modeling exercise.
5. On the basis of these two studies, the tentative conclusion is that a consistent set of data has been produced which can be used for the modeling of future JAERI irradiation.

ACKNOWLEDGEMENT

The authors wish to express their gratitude to Mr. O. Baba, Director of the Department of HTTR Project, Dr. K. Kunitomi, former head of the HTTR Reactor Engineering Division, members of the HTTR Reactor Engineering Division, for their encouragement of this study. The authors also appreciate Dr. K. Minato, Principal Engineer of Department of Materials Science, for his useful comments on this report.

REFERENCES

1. S. Saito, T. Tanaka, Y. Sudo, O. Baba, et al., "Design of High Temperature Engineering Test Reactor (HTTR)", *JAERI-1332* (1994).
2. K. Sawa, T. Tobita, H. Mogi, S. Shiozawa, et al., "Fabrication of the First-Loading Fuel of the High Temperature Engineering Test Reactor", *J. Nucl. Sci. Technol.*, Vol. 36, p. 683 (1999).
3. D. G. Martin, "Some Calculations of the Failure Statistics of Coated Fuel Particles", *Nucl. Technol.*, Vol. 42, p. 304 (1979).
4. K. Sawa and K. Minato, "An Investigation of Irradiation Performance of High Burnup HTGR Fuel", *J. Nucl. Sci. Technol.*, Vol. 36, p. 781 (1999).
5. K. Minato, K. Sawa, K. Fukuda, C. A. Baldwin, et al., "HRB-22 Capsule Irradiation Test for HTGR Fuel", *JAERI-Research 98-021* (1998).
6. K. Sawa, S. Shiozawa, K. Minato and K. Fukuda, "Development of a Coated Fuel Particle Failure Model under High Burnup Irradiation", *J. Nucl. Sci. Technol.*, Vol. 33, p. 712 (1996).
7. H. Walther, "On mathematical models for calculating the mechanical behaviour of coated particles", *Nucl. Eng. Des.* Vol. 18, p. 11 (1972).
8. K. Minato, K. Kikuchi, K. Sawa, T. Tobita, et al., "Preliminary Characterization of HTGR Fuel for HRB-22 Capsule Irradiation Test (JAERI/US DOE Collaborative Irradiation Test for HTGR Fuel)", *JAERI-Tech 95-056* (1996).
9. K. Minato, K. Sawa, T. Koya, T. Tomita, "Fission Product Release Behavior of Individual Coated Fuel Particles for High-temperature Gas-cooled Reactor", *Nucl. Technol.*, Vol. 31, p. 36 (2000).
10. K. Sawa, Private Communication (2000).

11. K. Bongartz, E. Gyarmati, H. Schuster and K. Täuber. *J. Nucl. Mater.* Vol. 62, p. 123 (1976).
12. D. G. Martin, “Pyrocarbon in High Temperature Nuclear Reactors” Chapter 7 of *Irradiation Damage in Graphite due to Fast Neutrons in Fission and Fusion Systems.* IAEA-TECDOC-1154 (September 2000).

Table 1 Dimensions of the irradiated coated fuel particles.

	HRB-22		91F-1A	
	Mean value (μm)	Standard deviation (μm)	Mean value (μm)	Standard deviation (μm)
Kernel diameter	544	9.1	551	9.9
Buffer thickness	97.4	13	97.3	12
IPyC thickness	32.9	3.4	32.1	3.4
SiC thickness	33.7	1.6	34.2	1.7
OPyC thickness	39.3	3.1	38.6	3.7

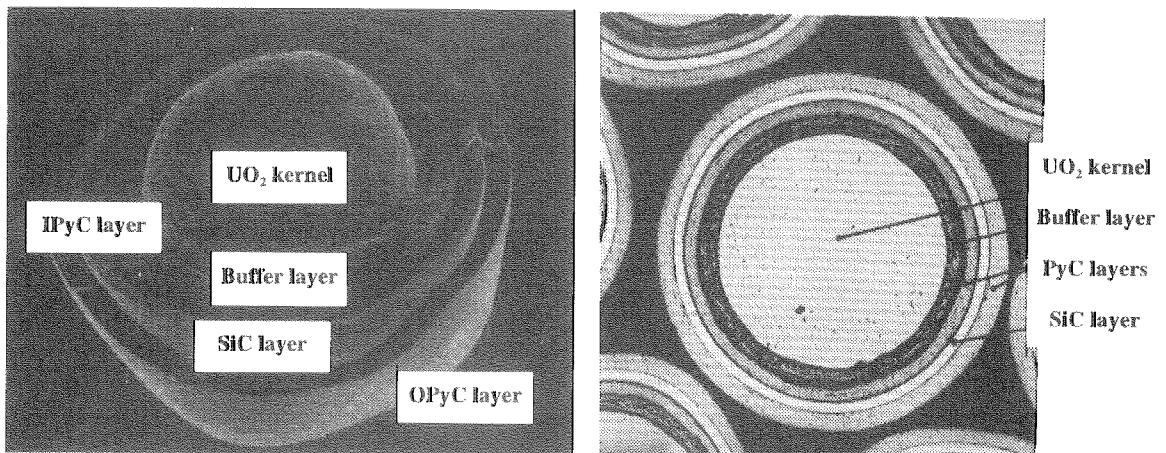


Fig. 1 TRISO-coated fuel particle.

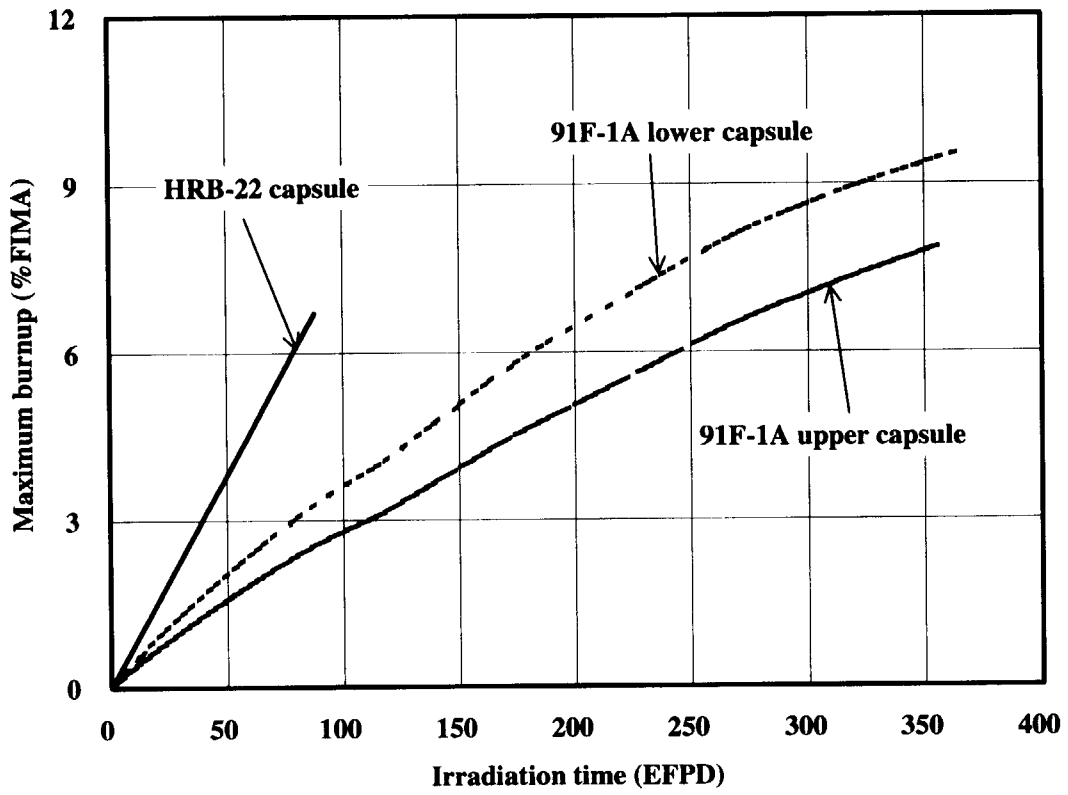


Fig.2 Burnups in irradiation tests.

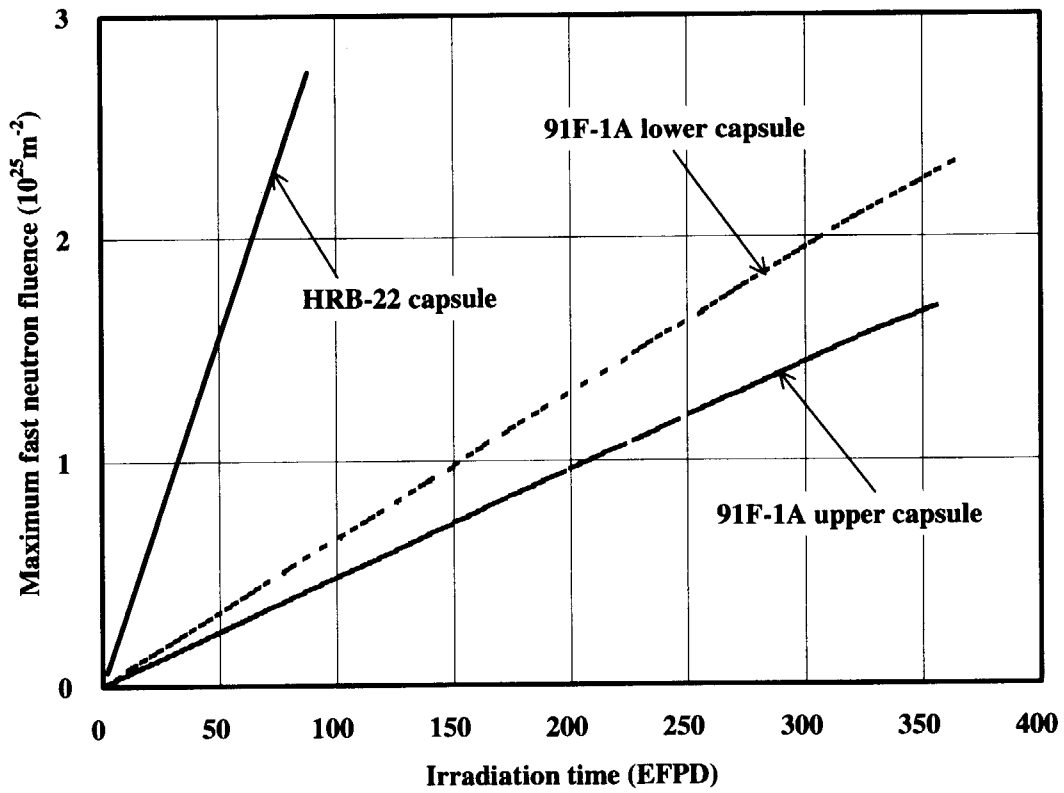


Fig.3 Fast neutron fluences in irradiation tests.

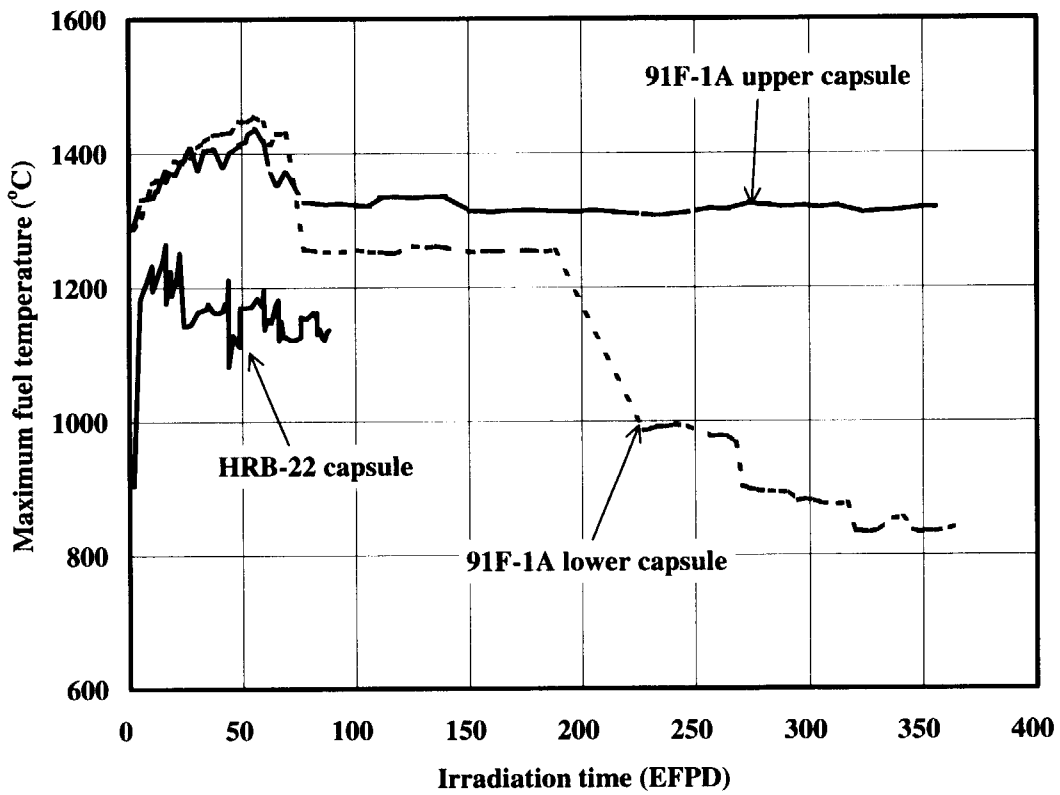


Fig.4 Maximum fuel temperatures in irradiation tests.

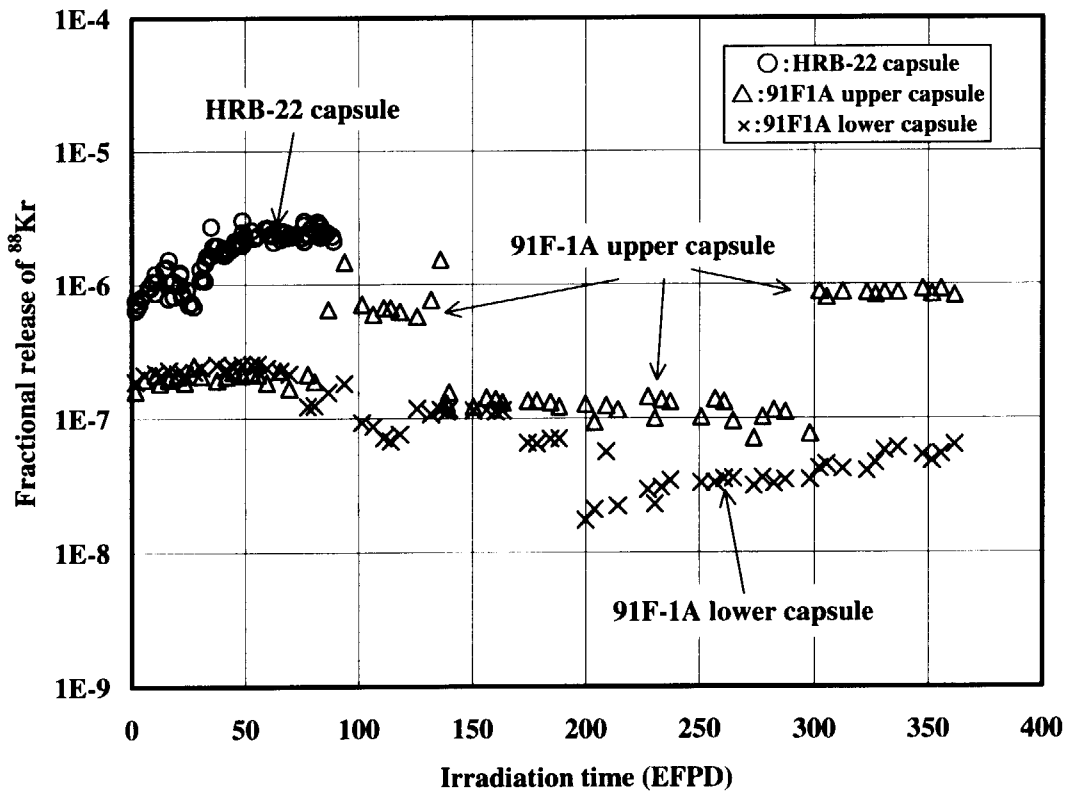


Fig. 5 Measured fractional releases in irradiation tests.

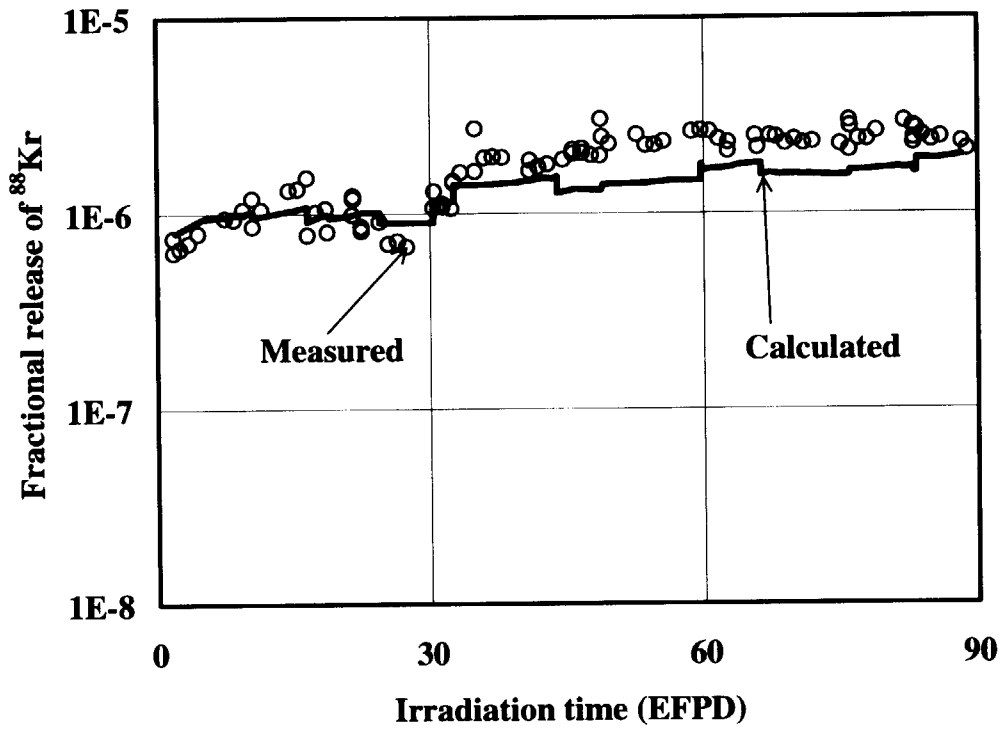


Fig. 6 Comparison of measured and calculated fractional releases in HRB-22 capsule irradiation test.

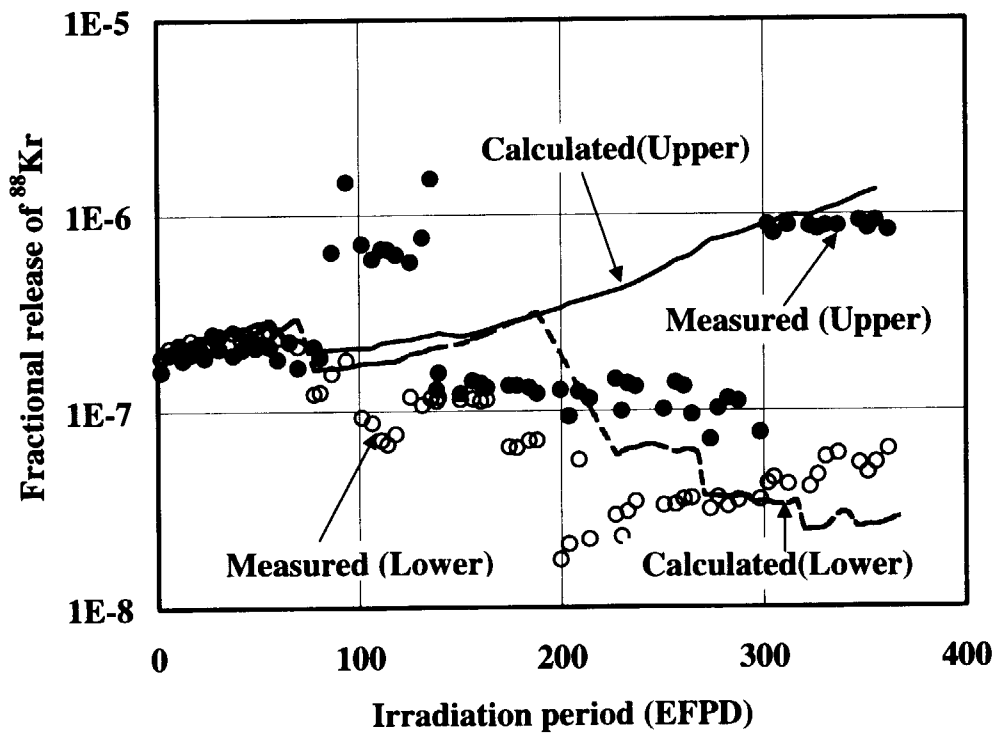


Fig. 7 Comparison of measured and calculated fractional releases in 91F-1A capsule irradiation test.

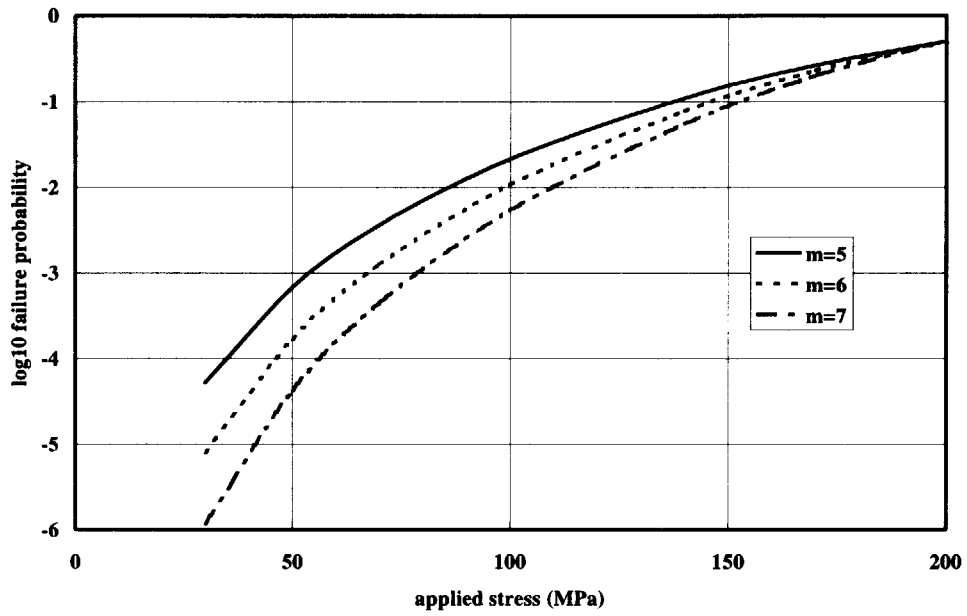


Fig. 8 Calculated failure probabilities in the HRB-22 capsule irradiation test as a function of Weibull modulus (mean strength = 200 MPa).

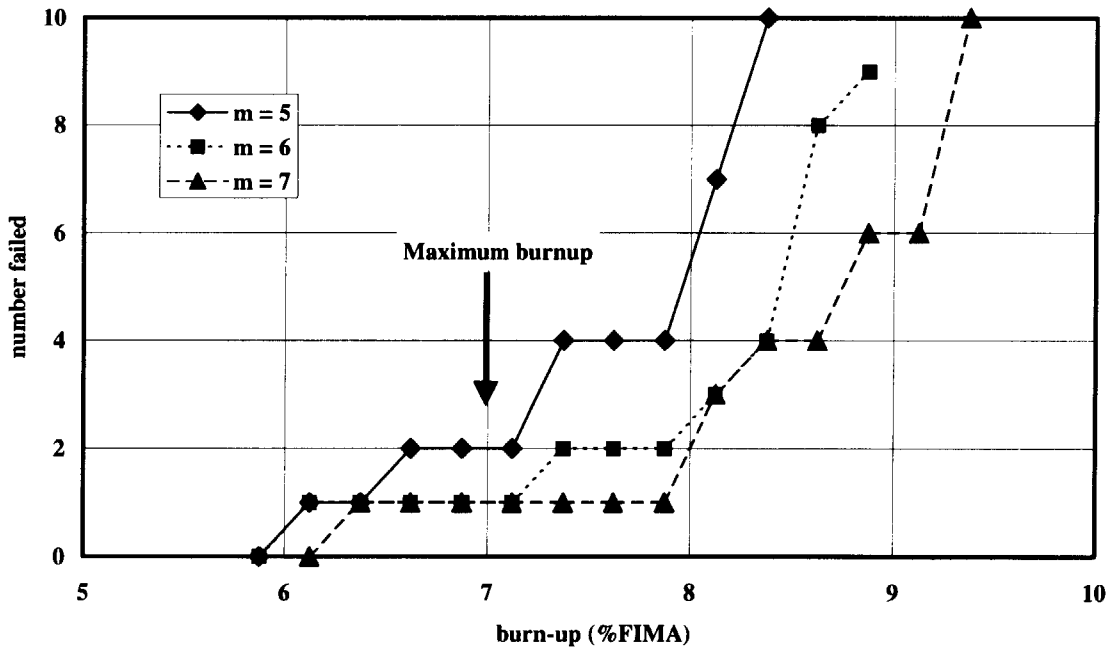


Fig. 9 Calculated number of additional failure during the HRB-22 capsule irradiation test as a function of Weibull modulus (mean strength = 200 MPa).

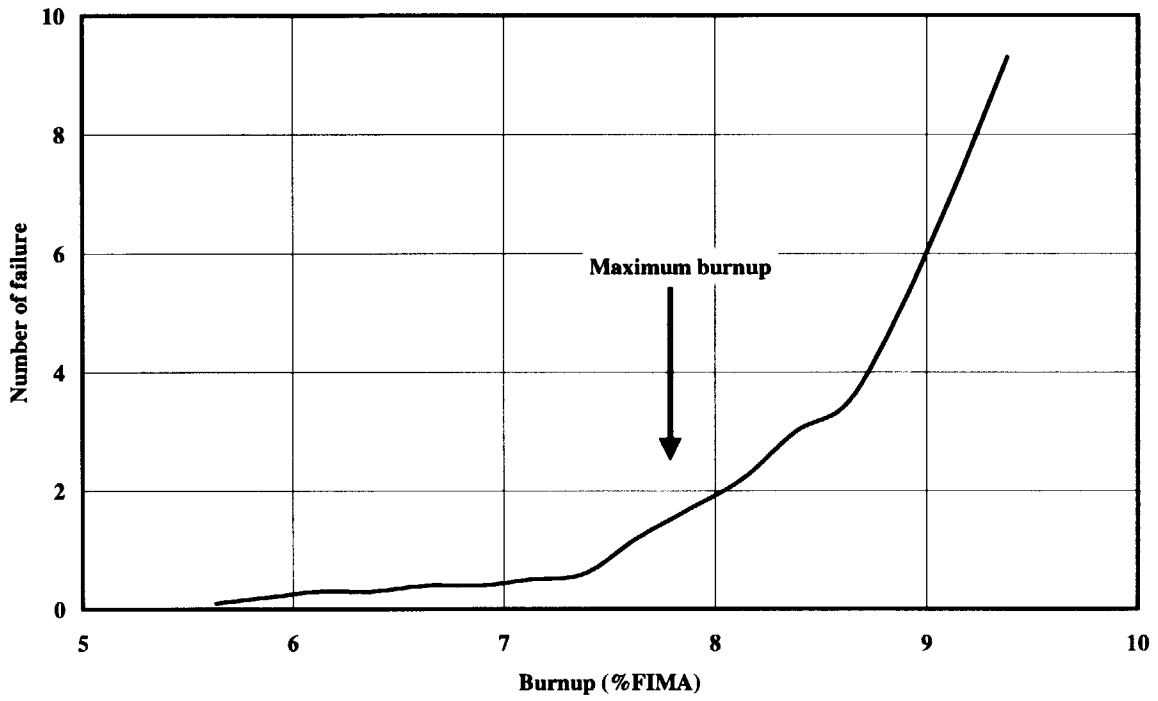


Fig. 10 Calculated number of additional failure during the 91F-1A upper capsule irradiation test.

This is a blank page.

国際単位系 (SI) と換算表

表1 SI基本単位および補助単位

量	名称	記号
長さ	メートル	m
質量	キログラム	kg
時間	秒	s
電流	アンペア	A
熱力学温度	ケルビン	K
物質質量	モル	mol
光度	カンデラ	cd
平面角	ラジアン	rad
立体角	ステラジアン	sr

表3 固有の名称をもつSI組立単位

量	名称	記号	他のSI単位による表現
周波数	ヘルツ	Hz	s ⁻¹
力	ニュートン	N	m·kg/s ²
圧力, 応力	パスカル	Pa	N/m ²
エネルギー, 仕事, 熱量	ジュール	J	N·m
工率, 放射束	ワット	W	J/s
電気量, 電荷	クーロン	C	A·s
電位, 電圧, 起電力	ボルト	V	W/A
静電容量	ファラド	F	C/V
電気抵抗	オーム	Ω	V/A
コンダクタンス	ジーメンズ	S	A/V
磁束	ウェーバ	Wb	V·s
磁束密度	テスラ	T	Wb/m ²
インダクタンス	ヘンリー	H	Wb/A
セルシウス温度	セルシウス度	°C	
光束度	ルーメン	lm	cd·sr
照射	ルクス	lx	lm/m ²
放射能	ベクレル	Bq	s ⁻¹
吸収線量	グレイ	Gy	J/kg
線量当量	シーベルト	Sv	J/kg

表2 SIと併用される単位

名称	記号
分, 時, 日	min, h, d
度, 分, 秒	°, ', "
リットル	l, L
トン	t
電子ボルト	eV
原子質量単位	u

1 eV = 1.60218 × 10⁻¹⁹ J

1 u = 1.66054 × 10⁻²⁷ kg

表4 SIと共に暫定的に維持される単位

名称	記号
オングストローム	Å
バール	bar
ガリ	Gal
キュリー	Ci
レントゲン	R
ラド	rad
レム	rem

1 Å = 0.1 nm = 10⁻¹⁰ m

1 b = 100 fm² = 10⁻²⁸ m²

1 bar = 0.1 MPa = 10⁵ Pa

1 Gal = 1 cm/s² = 10⁻² m/s²

1 Ci = 3.7 × 10¹⁰ Bq

1 R = 2.58 × 10⁻⁴ C/kg

1 rad = 1 cGy = 10⁻² Gy

1 rem = 1 cSv = 10⁻² Sv

表5 SI接頭語

倍数	接頭語	記号
10 ¹⁸	エクサ	E
10 ¹⁵	ペタ	P
10 ¹²	テラ	T
10 ⁹	ギガ	G
10 ⁶	メガ	M
10 ³	キロ	k
10 ²	ヘクト	h
10 ¹	デカ	da
10 ⁻¹	デシ	d
10 ⁻²	センチ	c
10 ⁻³	ミリ	m
10 ⁻⁶	マイクロ	μ
10 ⁻⁹	ナノ	n
10 ⁻¹²	ピコ	p
10 ⁻¹⁵	フェムト	f
10 ⁻¹⁸	アト	a

(注)

- 表1-5は「国際単位系」第5版、国際度量衡局 1985年刊行による。ただし、1 eV および 1 uの値はCODATAの1986年推奨値によった。
- 表4には海里、ノット、アール、ヘクタールも含まれているが日常の単位なのでここでは省略した。
- barは、JISでは流体の圧力を表わす場合に限り表2のカテゴリーに分類されている。
- EC閣僚理事会指令ではbar, barnおよび「血圧の単位」mmHgを表2のカテゴリーに入れている。

換算表

力	N (=10 ⁵ dyn)	kgf	lbf
	1	0.101972	0.224809
	9.80665	1	2.20462
	4.44822	0.453592	1

粘度 1 Pa·s (N·s/m²) = 10 P (ポアズ) (g/(cm·s))

動粘度 1 m²/s = 10⁴ St (ストークス) (cm²/s)

圧	MPa (=10 bar)	kgf/cm ²	atm	mmHg (Torr)	lbf/in ² (psi)
	1	10.1972	9.86923	7.50062 × 10 ³	145.038
力	0.0980665	1	0.967841	735.559	14.2233
	0.101325	1.03323	1	760	14.6959
	1.33322 × 10 ⁻⁴	1.35951 × 10 ⁻³	1.31579 × 10 ⁻³	1	1.93368 × 10 ⁻²
	6.89476 × 10 ⁻³	7.03070 × 10 ⁻²	6.80460 × 10 ⁻²	51.7149	1

エネルギー・仕事・熱量	J (=10 ⁷ erg)	kgf·m	kW·h	cal (計量法)	Btu	ft·lbf	eV	1 cal = 4.18605 J (計量法) = 4.184 J (熱化学) = 4.1855 J (15 °C) = 4.1868 J (国際蒸気表)
	1	0.101972	2.77778 × 10 ⁻⁷	0.238889	9.47813 × 10 ⁻⁴	0.737562	6.24150 × 10 ¹⁸	
	9.80665	1	2.72407 × 10 ⁻⁶	2.34270	9.29487 × 10 ⁻³	7.23301	6.12082 × 10 ¹⁹	
	3.6 × 10 ⁶	3.67098 × 10 ³	1	8.59999 × 10 ⁵	3412.13	2.65522 × 10 ⁶	2.24694 × 10 ²⁵	
	4.18605	0.426858	1.16279 × 10 ⁻⁶	1	3.96759 × 10 ⁻³	3.08747	2.61272 × 10 ¹⁹	仕事率 1 PS (仏馬力) = 75 kgf·m/s = 735.499 W
	1055.06	107.586	2.93072 × 10 ⁻⁴	252.042	1	778.172	6.58515 × 10 ²¹	
	1.35582	0.138255	3.76616 × 10 ⁻⁷	0.323890	1.28506 × 10 ⁻³	1	8.46233 × 10 ¹⁸	
	1.60218 × 10 ⁻¹⁹	1.63377 × 10 ⁻²⁰	4.45050 × 10 ⁻²⁶	3.82743 × 10 ⁻²⁰	1.51857 × 10 ⁻²²	1.18171 × 10 ⁻¹⁹	1	

放射能	Bq	Ci
	1	2.70270 × 10 ⁻¹¹
	3.7 × 10 ¹⁰	1

吸収線量	Gy	rad
	1	100
	0.01	1

照射線量	C/kg	R
	1	3876
	2.58 × 10 ⁻⁴	1

線量当量	Sv	rem
	1	100
	0.01	1

A Study of Fuel Failure Behavior in High Burnup HTGR Fuel — Analysis by STRESS3 and STAPLE Codes—